
DMWM: Dual-Mind World Model with Long-Term Imagination

Lingyi Wang¹ Rashed Shelim¹ Walid Saad¹ Naren Ramakrishnan²

Abstract

Imagination in world models is crucial for enabling agents to learn long-horizon policy in a sample-efficient manner. Existing recurrent state-space model (RSSM)-based world models depend on single-step statistical inference to capture the environment dynamics, and, hence, they are unable to perform long-term imagination tasks due to the accumulation of prediction errors. Inspired by the dual-process theory of human cognition, we propose a novel dual-mind world model (DMWM) framework that integrates logical reasoning to enable imagination with logical consistency. DMWM is composed of two components: an RSSM-based System 1 (RSSM-S1) component that handles state transitions in an intuitive manner and a logic-integrated neural network-based System 2 (LINN-S2) component that guides the imagination process through hierarchical deep logical reasoning. The inter-system feedback mechanism is designed to ensure that the imagination process follows the logical rules of the real environment. The proposed framework is evaluated on benchmark tasks that require long-term planning from the DMControl suite. Extensive experimental results demonstrate that the proposed framework yields significant improvements in terms of logical coherence, trial efficiency, data efficiency and long-term imagination over the state-of-the-art world models.

real-world interactions thus significantly improving data efficiency and minimizing trial-and-error costs. For complex tasks requiring long-term planning, imagination capabilities allow world models to evaluate the long-term consequences of diverse strategies and identify the optimal action plans. Consequently, the effectiveness of model-based decision-making approaches, such as model-based reinforcement learning (RL) (Hafner et al., 2019a; 2020; 2023; Wang et al., 2024) and model predictive control (MPC) (Hafner et al., 2019b; Hansen et al., 2022; SV et al., 2023), can heavily depend on the quality of their imagination abilities.

One of the most widely used frameworks for world models is the so-called recurrent state-space model (RSSM) (Hafner et al., 2019b; Zhu et al., 2020; Du et al., 2024) and its variants (Hansen et al., 2023; Sun et al., 2024) that combine deterministic recurrent structures with stochastic latent variables to model environmental dynamics in a compact latent space. By doing so, RSSM models can capture the sequential dependencies and uncertainty of their target environment. However, RSSM faces challenges in providing reliable, long-term predictions over extended imagination horizons due to the accumulation of prediction errors and the limitations of statistical inference (Ke et al., 2018; Simeonov et al., 2021; Clinton & Lieck, 2024). In particular, although existing RSSM-based solutions can generate accurate short-term predictions in a single-step manner, small errors inevitably propagate over longer time horizons (Lambert et al., 2021), gradually amplifying over each step and resulting in significant deviations between the imagined and actual states. Moreover, RSSM schemes often optimize state-space representations through reconstruction loss or regression. This approach can lead to overfitting to observed patterns and cannot properly capture latent dynamics (Lambert et al., 2021; Simeonov et al., 2021), particularly in complex, dynamic environments.

Several models have been proposed to enhance long-term planning. For instance, trajectory-based models (Lambert et al., 2021) learn long-term dynamics by directly predicting future states to reduce compounding errors compared to single-step prediction models. However, the absence of intermediate states impedes accurate action decisions, particularly in complex, high-precision tasks. Latent space-enhanced models (Ke et al., 2018; Simeonov et al., 2021) incorporate abstracted long-term information, such as high-

1. Introduction

Imagination is a core capability of world models that allows agents to predict and plan effectively within internal virtual environments by using real-world knowledge (Lin et al., 2020; Zhu et al., 2020; Mattes et al., 2023; Cohen et al., 2024). By predicting future scenarios in latent spaces, agents can evaluate potential outcomes without frequent

¹Department of Electrical and Computer Engineering, Virginia Tech, USA ²Department of Computer Science, Virginia Tech, USA.

level goals and global knowledge, to mitigate error propagation in each single-step prediction. However, these long-term planning approaches (Lambert et al., 2021; Ke et al., 2018; Simeonov et al., 2021) still rely on statistical inference and lack logical consistency along with interpretability over extended horizons.

Motivated by the challenges of long-term imagination and the limitations of existing long-term planning approaches, we propose a novel dual-mind world model (DMWM) framework based on the dual-process theory of human cognition (Frankish, 2010; Evans, 2003). The proposed DMWM framework can achieve reliable and efficient imagination by combining the complementary strengths of System 1 and System 2 learning processes (Hua & Zhang, 2022). By designing this framework, we make the following key contributions:

- We propose DMWM, a novel world model framework consisting of RSSM-based System 1 (RSSM-S1) component and logic-integrated neural network-based System 2 (LINN-S2) component inspired by the dual-process theory of human cognition. In DMWM, the RSSM-S1 component predicts the state transitions in a fast, intuitive-driven manner, while the LINN-S2 component guides the imagination process through logical reasoning at a higher level.
- In LINN-S2, we introduce logical regularization rules to conduct logical reasoning within the state and action spaces by using operations such as \wedge , \vee , \neg and \rightarrow . The logical rules allows the logical consistency and interpretability of the world model. Additionally, we propose a recursive logic reasoning framework that extends local reasoning into globally consistent long-term planning, enabling the modeling of logical sequence dependencies in complex tasks.
- We design an inter-system feedback mechanism. In particular, LINN-S2 provides logical constraints to guide RSSM-S1 so as to ensure that predicted sequences are consistent with domain-specific logical rules. For the feedback based on real-world data from RSSM-S1, it updates the domain-specific logics of LINN-S2, thereby allowing dynamic refinement and adaptation.
- We evaluate our proposed DMWM with actor-critic based RL and MPC in extensive experiments. The simulation results demonstrate that DMWM is able to respectively provide 14.3%, 5.5-fold, 32% and 120% improvement in logic consistency, trial efficiency, data efficiency and reliable imagination over extended horizon size compared to baselines in complex tasks.

2. Proposed DMWM Framework

In this section, we introduce the proposed DMWM framework with long-term imagination capabilities inspired by the

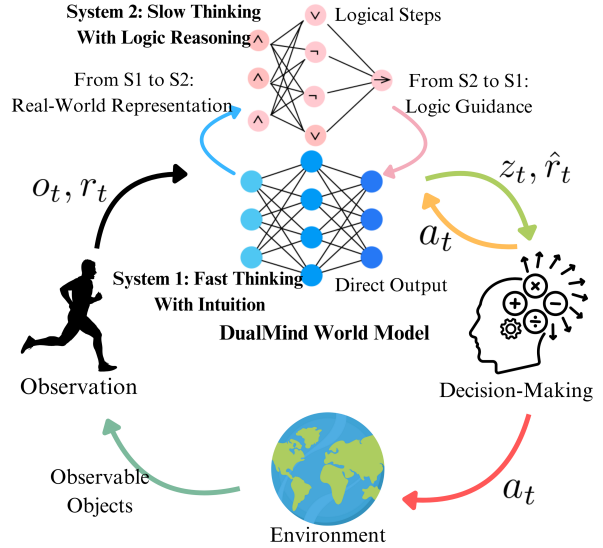


Figure 1. The pipeline of the proposed framework with DMWM.

dual-process theory of human cognition. DMWM consists of RSSM-S1 and LINN-S2. First, we introduce RSSM-S1, which builds upon the RSSM architecture to learn the environment dynamics in a latent space and perform fast, intuitive state representations and predictions. Next, based on the LINN, we introduce a novel LINN-S2 to capture the intricate logical relationships between the state space and the action space. By employing a hierarchical deep reasoning framework, LINN-S2 facilitates structured reasoning and enforces logical consistency over extended horizons. Finally, we provide an inter-system feedback mechanism. The pipeline of the proposed DMWM framework is shown in Figure 1.

2.1. RSSM-based System 1

The RSSM-S1 component is based on DreamerV3 (Hafner et al., 2023).

$$\begin{aligned}
 \text{Deterministic State: } & h_t = f_\varphi(h_{t-1}, z_{t-1}, a_{t-1}), \\
 \text{Encoder: } & z_t \sim q_\varphi(z_t | h_t, o_t), \\
 \text{Stochastic State: } & \hat{z}_t \sim p_\varphi(\hat{z}_t | h_t), \\
 \text{Reward Predictor: } & \hat{r}_t \sim p_\varphi(\hat{r}_t | h_t, z_t), \\
 \text{Decoder: } & \hat{o}_t \sim p_\varphi(\hat{o}_t | h_t, z_t),
 \end{aligned}$$

with the deterministic state h_t , observation o_t , predicted observation \hat{o}_t , stochastic state z_t , predicted stochastic state \hat{z}_t , action a_t and the predicted reward \hat{r}_t at time step t . RSSM-S1 achieves an effective balance between deterministic and stochastic states, enabling efficient data-driven prediction similar to the intuitive and automatic processes of System 1. The deterministic state captures data patterns, and the stochastic state models inherent uncertainty and variability for dynamic and complex environments.

System 1 loss. RSSM-S1 is optimized by using the loss functions of DreamerV3.

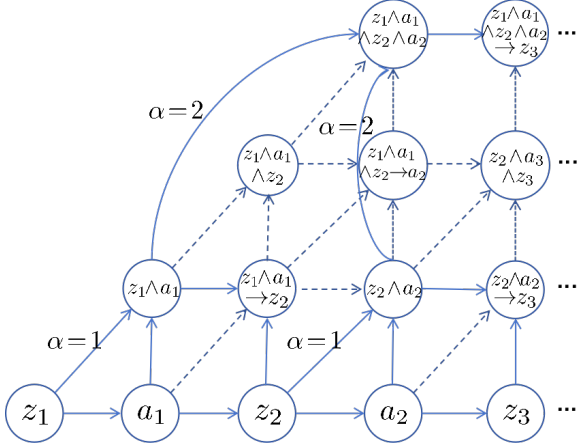


Figure 2. Logic reasoning with LINN-S2 for DMWM

$$\begin{aligned}
 \mathcal{L}_{S1}(\varphi) &= \mathcal{L}_{\text{pred}}(\varphi) + \varpi_{\text{dyn}} \mathcal{L}_{\text{dyn}}(\varphi) + \varpi_{\text{rep}} \mathcal{L}_{\text{rep}}(\varphi), \\
 \mathcal{L}_{\text{pred}}(\varphi) &= -\ln p_{\varphi}(o_t | z_t, h_t) - \ln p_{\varphi}(r_t | z_t, h_t) \\
 &\quad - \ln p_{\varphi}(c_t | z_t, h_t), \\
 \mathcal{L}_{\text{dyn}}(\varphi) &= \text{KL}[\text{sg}(q_{\varphi}(z_t | h_t, o_t)) \| p_{\varphi}(z_t | h_t)], \\
 \mathcal{L}_{\text{rep}}(\varphi) &= \text{KL}[q_{\varphi}(z_t | h_t, o_t) \| \text{sg}(p_{\varphi}(z_t | h_t))],
 \end{aligned} \tag{1}$$

where ϖ_{dyn} and ϖ_{rep} are respectively the weight factors of the dynamic loss \mathcal{L}_{dyn} and the representation loss \mathcal{L}_{rep} , and $\text{sg}(\cdot)$ represents the stop-gradient operator.

System 1 limitations. The RSSM can be regarded as a computational counterpart of System 1 within dual-process theories of cognition, doing well in fast, intuitive-driven reasoning. However, it is inherently constrained by two critical limitations: *the absence of explicit logical reasoning* and *the inability to maintain coherence over extended temporal horizons*. While RSSM-S1 enables efficient and immediate response through pattern recognition and intuitive prediction, these strengths come at the cost of enforcing logical consistency or inferring causal relationships in complex scenarios. Moreover, RSSM-S1’s focus on short-term processing limits its ability to integrate information across long periods, resulting in fragmented or inconsistent predictions in tasks that demand global planning or long-term foresight. These inherent limitations demonstrate the need to complement the capabilities of RSSM-S1 with mechanisms similar to System 2, which does well in structured reasoning and sustained temporal coherence, to construct a more robust and comprehensive cognitive world model framework.

2.2. Logic-integrated neural network-based System 2

Next, we introduce the LINN-S2 component whose deep logical reasoning is illustrated in Figure 2. In LINN-S2, the states and actions are encoded as logic vector inputs, enabling logical deduction through operations such as negation (\neg), conjunction (\wedge), disjunction (\vee), and implication (\rightarrow). To establish these logical operations, the LINN framework

(Shi et al., 2020) serves as the foundational module for capturing and reasoning about structural logical relationships between the state embedding space and the action embedding space within the world model. To further enhance the logical reasoning capabilities, we incorporate a set of regularization rules specifically designed for implication-based operations.

Neural modules for basic logic operations. In logical reasoning for world models, it is essential to uncover structural information and semantic relationships across different embedding spaces, specifically the action space and the state space. (Shi et al., 2020) proposed a straightforward concatenation-based method for LINN but it limits that input vectors are from the same source space. Moreover, the straightforward concatenation-based method overlooks the semantic disparities between states and actions, risking the loss of critical information and failing to capture complex cross-space logical relationships.

To address the need for cross-space logical reasoning in world models, we propose to explore the action embeddings and apply the Kronecker product for cross-space feature alignment, which preserves logic integrity and captures second-order relationships. The state (imagination) logical embedding v and the state logical embedding m are obtained with multilayer perceptron (MLP) by

$$v = \mathbf{W}_2^s f(\mathbf{W}_1^s(z) + \mathbf{b}_w^s), m = \mathbf{W}_2^a f(\mathbf{W}_1^a(z \oplus a) + \mathbf{b}_w^a), \tag{2}$$

where \oplus is the operation of vector concatenation, and $z \oplus a$ aims to capture the action logic within the state context. The formulations of operations (AND, OR, NOT) are given as follows

$$\text{AND}(v, m) = \mathbf{W}_2^a f(\mathbf{W}_1^d(v \oplus m) + \mathbf{b}_w^d) + \text{Conv2D}(v \otimes m, \mathbf{K}^d) + \mathbf{b}_k^d, \tag{3}$$

$$\text{OR}(v, m) = \mathbf{W}_2^o f(\mathbf{W}_1^o(v \oplus m) + \mathbf{b}_w^o) + \text{Conv2D}(v \otimes m, \mathbf{K}^o) + \mathbf{b}_k^o, \tag{4}$$

$$\text{NOT}(v) = v + \mathbf{W}_2^n f(\mathbf{W}_1^n v + \mathbf{b}_w^n), \tag{5}$$

where $v \in \mathbb{R}^d$, $m \in \mathbb{R}^d$, $\mathbf{W}_1^l \in \mathbb{R}^{d \times 2d}$, $\mathbf{W}_2^l \in \mathbb{R}^{d \times d}$, $\mathbf{b}_w^l \in \mathbb{R}^d$, $\mathbf{b}_k^l \in \mathbb{R}^d$ are the parameters of the logical neural networks, $l \in \{d, o, n\}$, $\text{Conv2D}(\cdot)$ represents the convolution neural network, \mathbf{K} is the convolution core, \otimes is the operation of Kronecker product, and $f(\cdot)$ is the activation function.

It is clear that logical operations capture intricate logical correlations that cannot be fully encapsulated by the geometric properties of the embedding space. For instance, the logical independence in $\text{NOT}(v)$, reflected in the relationship between v and $\neg v$, does not correspond precisely to vector orthogonality. Logical operations are governed by logical

axioms (e.g., identity, annihilator, and complementation), which impose algebraic constraints that transcend purely geometric interpretations, which are introduced in the logic regularization part.

Implication relationship for state reasoning. Based on the basic logical operations (AND, OR, NOT), we implement the implication operation ($p_\varphi \rightarrow q_\varphi$) to enable logical reasoning within the state and action logical embedding spaces. The implication operation is critical for assessing the rationality of a predicted state given the current imagination and action embeddings, which is derived through the equivalence relationship:

$$p \rightarrow q \iff \neg p \vee q. \quad (6)$$

Hence, the operation IMPLY for $v \rightarrow m$ can be realized based on the fundamental operations of negation (\neg) and conjunction (\wedge), which is represented by

$$\text{IMPLY}(v, m) = \text{OR}(\text{NOT}(v), m). \quad (7)$$

Logical regularizations. To ensure that neural modules accurately perform logical operations, (Shi et al., 2020) introduced logic regularizers $\{r_i\}$ that enforce adherence to fundamental logical rules, thereby constraining module behavior. While neural networks can implicitly learn logical operations from data, the explicit incorporation of logical constraints improves model consistency, interpretability, and robustness while maintaining efficient neural computation. Derived from principles of AND, OR, and NOT, logic regularizers establish a unified inference framework with fundamental and advanced operations. This approach aligns model outputs with human-understandable reasoning, bridging neural networks and formal logic, and enabling effective learning, representation, and inference of logical formulas for interpretable reasoning in world models.

We extend the foundational framework of logical regularization in (Shi et al., 2020) by introducing implication regularizers to address advanced logical rules. As summarized in Table 1, the implication rules refine basic logical structures to handle intricate constructs. By explicitly encoding principles such as *contraposition* ($w \rightarrow v \equiv \neg v \rightarrow \neg w$) and *complementation* ($w \rightarrow \neg w \equiv \neg w$), LINN-S2 improves its capacity to manage compound logical expressions while ensuring consistency across implication operations.

The logical regularizers for IMPLY (r_{11} - r_{14}), partial depicted in Table 1, combined with the basic logical regularizers for AND, OR, and NOT (r_1 - r_{10}), collectively define the regularization loss function L_r , which is expressed as

$$\mathcal{L}_{\text{reg}} = \frac{1}{N_r} \sum_i r_i, \quad (8)$$

where r_i represents individual logical regularizers and N_r

presents the total number of the regularizers. The complete table of the logical regularizers is given in Appendix F.

Symbolic representation of deep logical reasoning. In this part, we present the symbolic representation of LINN-S2 for deep logical reasoning. Specifically, the logical reasoning process is formalized by using symbolic logic to represent logical relationships in sequences. By leveraging logical operations (\wedge, \rightarrow), LINN-S2 constructs a hierarchical logical reasoning framework, facilitating systematic and interpretable reasoning over sequential dependencies. The framework of the hierarchical logical reasoning is illustrated in Figure 2, and three detailed process procedures are given as follows.

1) *Local logical composition*: Each state (imagination) logical embedding v_t and action logical embedding m_t are combined by using the logical conjunction (\wedge) to capture the intrinsic logic relationship

$$c_t : v_t \wedge m_t, \quad \forall t < T. \quad (9)$$

The composition c_t establishes localized logical features based on the existing v_t and m_t .

2) *Recursive implication reasoning*: To ensure logical consistency across states (imagination), each composition (c_t) undergoes an implication operation (\rightarrow) that aligns the logical information with the subsequent state (imagination)

$$\phi_t : c_t \rightarrow z_{t+1}, \quad \forall t < T. \quad (10)$$

The recursive formulation (9) encodes sequential dependencies and enforces consistency in predictive state transitions across the hierarchy. However, ϕ_t provides only single-step logical inference, and it lacks reasoning depth and comprehensiveness. To address this limitation, we propose incorporating deterministic historical information into the logical reasoning framework. The deep recursive implication reasoning is represented by

$$\phi_t^\alpha : c_{t-\alpha} \cdots \wedge c_{t-1} \wedge c_t \rightarrow z_{t+1}, \quad \forall \alpha < t < T, \quad (11)$$

where α is the inference depth. In complex scenarios with long-term dependencies, the model utilizes logical relationships from past states to ensure coherent reasoning. Capturing logic across time steps retains historical information, strengthens sequential dependencies and enhances global consistency. This prevents inference bias from information loss during multi-step reasoning and ensures the reliability of long-term imagination.

3) *Global logical chain*: The global reasoning process integrates local consistency and recursive reasoning into a unified global logical chain L_T within the time period T

$$L_T^\alpha = \phi_1^\alpha \wedge \phi_2^\alpha \wedge \phi_3^\alpha \cdots \phi_{T-1}^\alpha \rightarrow \mathbf{T}, \quad (12)$$

where \mathbf{T} represents the terminal consistency condition, ensuring that the state (imagination) sequences align with the

Table 1. Partial Logical Regularizers and Rules for Implication \rightarrow

	Logical Rule	Equation	Logic Regularizer r_i
IMPLY	Identity	$w \rightarrow \mathbf{T} = \mathbf{T}$	$r_{11} = \sum_{w \in \mathcal{W}} 1 - \text{Sim}(\text{OR}(\text{NOT}(w), \mathbf{T}), \mathbf{T})$
	Annihilator	$w \rightarrow \mathbf{F} = \neg w$	$r_{12} = \sum_{w \in \mathcal{W}} 1 - \text{Sim}(\text{OR}(\text{NOT}(w), \mathbf{F}), \text{NOT}(w))$
	Idempotence	$w \rightarrow w = \mathbf{T}$	$r_{13} = \sum_{w \in \mathcal{W}} 1 - \text{Sim}(\text{OR}(\text{NOT}(w), w), \mathbf{T})$
	Complementation	$w \rightarrow \neg w \equiv \neg w$	$r_{14} = \sum_{w \in \mathcal{W}} 1 - \text{Sim}(\text{OR}(\text{NOT}(w), \text{NOT}(w)), \text{NOT}(w))$

reasoning objectives. This formulation consolidates local information into a globally consistent reasoning framework.

In this way, LINN-S2 enhances the formal interpretation and mathematical rigor of world models along with several key features. First, the hierarchical structure encodes deep logical reasoning as a layered process, which allows logical consistency between state and action representations. Second, logical composition leverages logical operations for binding states and actions in a logical manner. This composition facilitates formal logic principles and enables modular, interpretable reasoning. Finally, the recursive implication structure ensures robustness and interpretability for long-term imagination.

System 2 loss. The loss function of the logic reasoning with the inference depth α is represented by

$$\begin{aligned} \mathcal{L}_{\log}^{\alpha} &= \frac{1}{T-1} \sum_t \mathcal{S}(\phi_t^{\alpha}, \mathbf{T}) - \mathcal{S}(\phi_t^{\alpha}, \mathbf{F}) \\ &= \frac{1}{T-1} \sum_t \mathcal{S}(\phi_t^{\alpha}, \mathbf{T}) - \mathcal{S}(\phi_t^{\alpha}, \text{NOT}(\mathbf{T})), \end{aligned} \quad (13)$$

where the \mathcal{S} is the logic similarity metric that takes value between 0 and 1. Here, we use the vector cosine similarity since the logical information of action and state spaces has been aligned in the logical vector space, given by

$$\mathcal{S}(v, m) = \sigma \left(\kappa \frac{v \cdot m}{\|v\| \|m\|} \right). \quad (14)$$

To ensure the logical consistency of basic operations of AND and OR by order-independence, i.e., $v \wedge m = m \wedge v$ and $v \vee m = m \vee v$, the inputs of AND and OR are randomly disrupted. Moreover, the ℓ_2 -regularization term \mathcal{L}_v (Shi et al., 2020) is employed to prevent the vector lengths from exploding, which could otherwise lead to trivial solutions (e.g., logical rules becoming ineffective) during optimization, and constraint on the model parameters to mitigate the risk of overfitting, represented by

$$\mathcal{L}_{\ell_2} = \sum_{v \in \mathcal{V}} \|v\|_F^2 + \sum_{m \in \mathcal{M}} \|m\|_F^2 + \sum_{w \in \mathcal{W}} \|w\|_F^2, \quad (15)$$

where \mathcal{W} represents the model parameters of LINN-S2. The loss function of System 2 is expressed as

$$\mathcal{L}_{S2}(w) = \sum_{\alpha=0}^{\Lambda} \mathcal{L}_{\log}^{\alpha} + \beta_{\text{reg}} \mathcal{L}_{\text{reg}} + \beta_{\ell_2} \mathcal{L}_{\ell_2}, \quad (16)$$

where β_{reg} and β_{ℓ_2} represents the weight factors, and Λ denotes the maximum reasoning depth.

2.3. Inter-System Feedback Mechanisms

Feedback from S1 to S2. During the real-environment interactions, LINN-S2 updates the domain-specific logical relationships by using the actual state transitions from RSSM-S1. In particular, the state-action sequence $\{z_t, a_t, z_{t+1}\}_{t=0}^T$ generated by RSSM-S1 based on the observations $\{o_t\}_{t=0}^{T+1}$ serves as the labeled data, which is fed into LINN-S2 with the objective of minimizing the inference loss (12).

Feedback from S2 to S1. To embed LINN-S2-inspired logical reasoning into RSSM-S1, we propose a logic feedback that utilizes LINN-S2’s logical consistency mechanisms to guide RSSM-S1. By unifying high-level logical structures with low-level representations, the approach fosters a more robust and coherent model for imagination. We particularly introduce the logical rule and rederive the variational evidence lower bound (ELBO) (Hafner et al., 2019a) with a logic inference term.

$$p_{\varphi}(o_{1:T}, z_{1:T} | a_{1:T}) = \prod_{t=1}^T p_{\varphi}(o_t | z_t) \tilde{p}_{\phi}(z_t | z_{t-1}, a_{t-1}), \quad (17)$$

where $\tilde{p}_{\phi}(z_t | z_{t-1}, a_{t-1}) \propto p_{\varphi}(z_t | z_{t-1}, a_{t-1}) \cdot \mathcal{C}(\phi(z_t, z_{t-1}, a_{t-1}))$ and $\mathcal{C}(\phi)$ is the logical consistency function that measures whether the logical rule ϕ is satisfied by imagination. The ELBO of the observation loss can be expressed as (Derivation in Appendix E)

$$\begin{aligned} \ln p_{\varphi}(o_{1:T} | a_{1:T}) &= \int p_{\varphi}(o_{1:T}, z_{1:T} | a_{1:T}) dz_{1:T} \\ &\geq \sum_{t=1}^T \left(\underbrace{\mathbb{E}_{q_1} [\ln p_{\varphi}(o_t | z_t)]}_{\text{Decoding}} + \underbrace{\mathbb{E}_{q_1} [\ln \mathcal{C}(\phi(z_t, z_{t-1}, a_{t-1}))]}_{\text{Logic Inference}} \right) \\ &\quad - \underbrace{\mathbb{E}_{q_2} [\text{KL} [q_{\varphi}(z_t | o_{\leq t}, a_{< t}) \| p_{\varphi}(z_t | z_{t-1}, a_{t-1})]}]_{\text{Prediction}}. \end{aligned}$$

where $q_1 = q_{\varphi}(z_t | o_{\leq t}, a_{< t})$ and $q_2 = q_{\varphi}(z_{t-1} | o_{\leq t-1}, a_{< t-1})$. The approximate state priors can be obtained by past observations and actions with the encoder

$$q_{\varphi}(z_{1:T} | o_{1:T}, a_{1:T}) = \prod_{t=1}^T q_{\varphi}(z_t | h_t, o_t). \quad (18)$$

3. Experimental Results and Analysis

In this section, we conduct extensive experiments to address the following key questions: (a) Can our model effectively capture logical relationships in dynamic environments?, (b) Does enhanced logical consistency enable our model to achieve higher task rewards under limited environment trials and data?, and (c) Over an extended horizon, can our model generate reliable long-term imagination?

Experimental setup. The training environments consist of 20 continuous control tasks from DeepMind control (DMC) suite. We evaluate DMWM using two model-based decision-making approaches: An actor-critic reinforcement learning method and a gradient-based model predictive control (Grad-MPC) approach (SV et al., 2023), referred to as DMWM-AC and DMWM-GD, respectively. Training details for DMWM-AC and DMWM-GD are provided in Appendix B. For comparison purposes and benchmarking, we include DreamerV3 (Hafner et al., 2023) and Dreamer-enabled Grad-MPC (SV et al., 2023) as baselines. To highlight the limitations of using a single RSSM for world cognition, we compare our method against two state-of-the-art RSSM variants: Hieros (Mattes et al., 2023) and HRSSM (Sun et al., 2024). HRSSM improves representation robustness via masking and bisimulation to mitigate visual noise interference, while Hieros enhances long-term modeling and exploration efficiency through S5WM and hierarchical strategies. Details on environment and model settings are provided in Appendix C.

Logical consistency. Figure 3 shows the logical correlations between individual state-action pairs ($s_i \wedge a_j$) and the target state (s_{30}). The diagonal shows strong correlations for one-step pairs $s_i \wedge a_i \rightarrow s_{30}$, which is the key path of localized reasoning. The off-diagonal elements show interdependency across different state-action pairs ($s_i \wedge a_j, i \neq j$) that propagate global logical information. The observed patterns highlight the need for deep logical reasoning to capture both short-term and long-term logical dependencies.

Table 2 compares the logical consistency of our proposed DMWM against various RSSM baselines on DMC tasks. Logical consistency data for 20 tasks with different horizon sizes is provided in Appendix G.1. The proposed DMWM achieves state-of-the-art logical consistency in both mean logic loss and stability across all DMC environments. DMWM respectively achieves 14.3%, 2.6% and 3.3% improvement of logic consistency compared to Dreamer, Hieros, and HRSSM. For instance, while the masking and hierarchical strategies in Hieros and HRSSM can reduce single-step propagation errors by mitigating environment noise, they still have difficulty in addressing long-term imagination due to predictive deviation in statistical inference and error accumulation. This highlights the limitations of

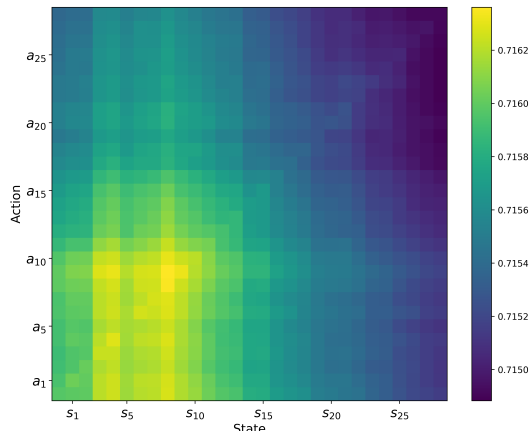


Figure 3. Heatmap of deep logic correlations for sequential imagination $s_0 \wedge a_0 \wedge \dots \wedge s_{29} \wedge a_{29} \rightarrow s_{30}$ with reasoning depth $\alpha = 30$. The horizontal axis indicates the past states s_j and the vertical axis indicates past actions a_j . The color of points represents the logical strength of state-action pairs to the long-term reasoning process.

relying solely on System 1 and the need for logical consistency from System 2 for robust long-term imagination.

Trial efficiency. Figure 4 presents test returns under limited environment trials. The number of environment trials serves as the x-axis to quantify exploration efficiency by measuring performance under the same environment interaction opportunities, which is a crucial factor for real-world applications and high-cost simulations. The complete results for 20 DMC tasks under limited environment trials are provided in Appendix G.2. The results show that DMWM-AC and DMWM-MPC significantly outperform baseline methods across most tasks with limited environment trials, particularly in complex environments such as Cheetah Run, Finger Turn Hard, and Quadraped Run. In contrast, Dreamer and GD-MPC exhibit limited performance in high-dimensional control tasks with lower learning efficiency and stability. As shown in Figure 4, DMWM approaches achieve an average 5.5-fold improvement in test return under limited environment trials under limited environment trials compared to baseline methods. These observations highlight that leveraging logical information from the environment enhances exploration efficiency, especially in complex tasks, enhancing DMWM’s capability in long-term imagination.

Data efficiency. Figure 5 presents test results under limited environment steps for the purpose of quantifying the data efficiency. The complete results for 20 tasks under limited environment steps are provided in Appendix G.3. DMWM approaches consistently outperform Dreamer and GD-MPC across most tasks in terms of convergence speed and final returns, particularly in high-dimensional dynamics such as Cheetah Run and Quadraped Run. These results highlight DMWM’s superior long-term planning and dynamic modeling capabilities, enabling more efficient utilization of environment data. In tasks that demand simple

Table 2. Performance comparison of our approach with various baselines on DMC tasks in terms of logic consistency. The mean and variance of logical consistency are reported over 100 test episodes with the horizon size $H = 30$. Complete results of logical consistency over 20 tasks with varying horizon size are concluded in Appendix G.1.

Env	Dreamer	Hieros	HRSSM	DMWM (Proposed)
Cartpole Balance	0.683 ± 0.057	0.711 ± 0.032	0.713 ± 0.041	0.727 ± 0.023
Pendulum Swingup	0.611 ± 0.137	0.709 ± 0.054	0.699 ± 0.079	0.730 ± 0.037
Reacher Hard	0.608 ± 0.121	0.702 ± 0.062	0.703 ± 0.072	0.730 ± 0.042
Finger Turn Hard	0.627 ± 0.131	0.698 ± 0.061	0.703 ± 0.073	0.725 ± 0.029
Cheetah Run	0.643 ± 0.131	0.689 ± 0.113	0.695 ± 0.087	0.725 ± 0.049
Cup Catch	0.652 ± 0.087	0.701 ± 0.072	0.714 ± 0.061	0.728 ± 0.021
Walker Walk	0.612 ± 0.140	0.696 ± 0.063	0.701 ± 0.073	0.730 ± 0.034
Quadruped Walk	0.656 ± 0.092	0.701 ± 0.067	0.703 ± 0.072	0.723 ± 0.039
Hopper Hop	0.633 ± 0.127	0.704 ± 0.087	0.701 ± 0.092	0.722 ± 0.038

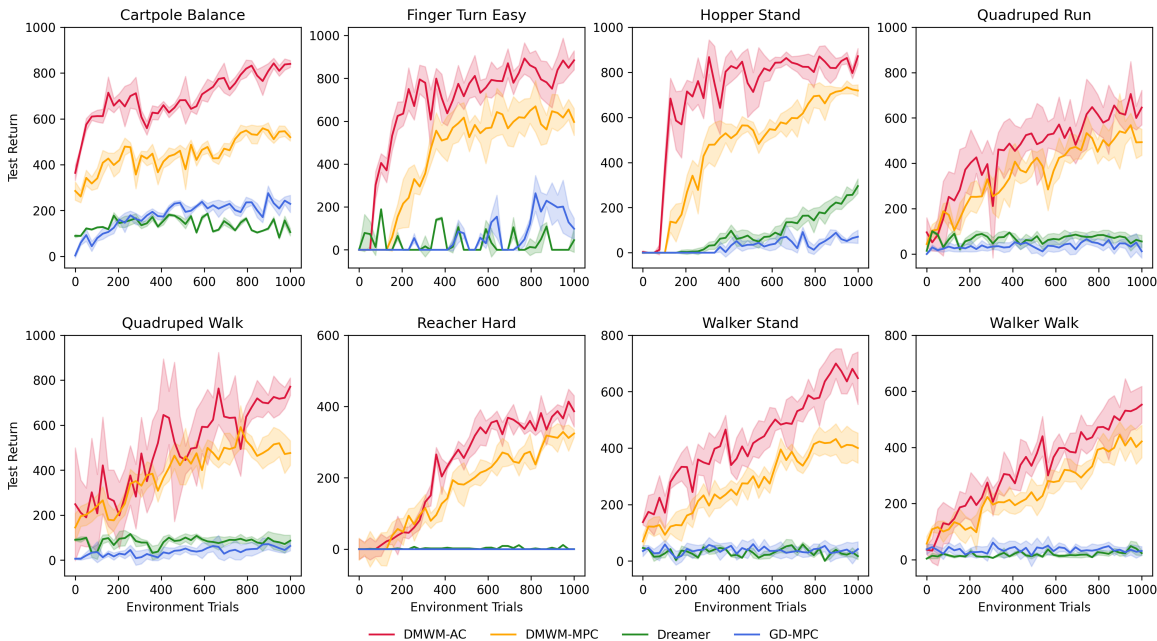


Figure 4. Performance comparison of results on 8 DMC tasks under limited environment trials, where the standard error is shaded in the distraction setting. The horizontal axis indicates the number of times that models explore the environments. The vertical axis indicates the average return over 100 test episodes. Complete results on 20 DMC tasks under limited environment interactions are concluded in Appendix G.2.

dynamic modeling like Cartpole Balance and Cup Catch, all methods converge rapidly. In contrast, for complex tasks like Reacher Hard and Hopper Hop, DMWM approaches achieve stable performance and an average improvement of 32% in test return under limited data compared to Dreamer and GD-MPC.

Imagination ability over extended horizon size. As shown in Figure 6, although a long-term prediction horizon introduces cumulative errors, DMWM-AC and DMWM-MPC consistently achieve high returns across most tasks and remain stable even over extended horizons. In stability-critical tasks such as Cartpole Balance and Pendulum Swingup, DMWM maintains strong performance across a wide range of prediction horizons, whereas Dreamer and GD-MPC are more susceptible to degradation due to prediction errors. For extended horizon size of $H > 30$ in complex tasks,

DMWM approaches achieve an average 120% improvement in test return compared to Dreamer and GD-MPC. These results emphasize the crucial role of logical reasoning in long-term imagination. Across most tasks, DMWM demonstrates superior performance over long-term horizons.

4. Conclusion and Limitations

Conclusion. In this paper, we have proposed DMWM, a novel world model framework for reliable long-term imagination that combines the fast, intuitive-driven RSSM-S1 with the structured, logic-driven inference of LINN. The feedback mechanisms between the two systems enhanced the logic coherence and adaptability. Extensive evaluations across diverse benchmarks demonstrated significant improvements in logical consistency, data-efficiency and reliable imagination over extended horizon size.

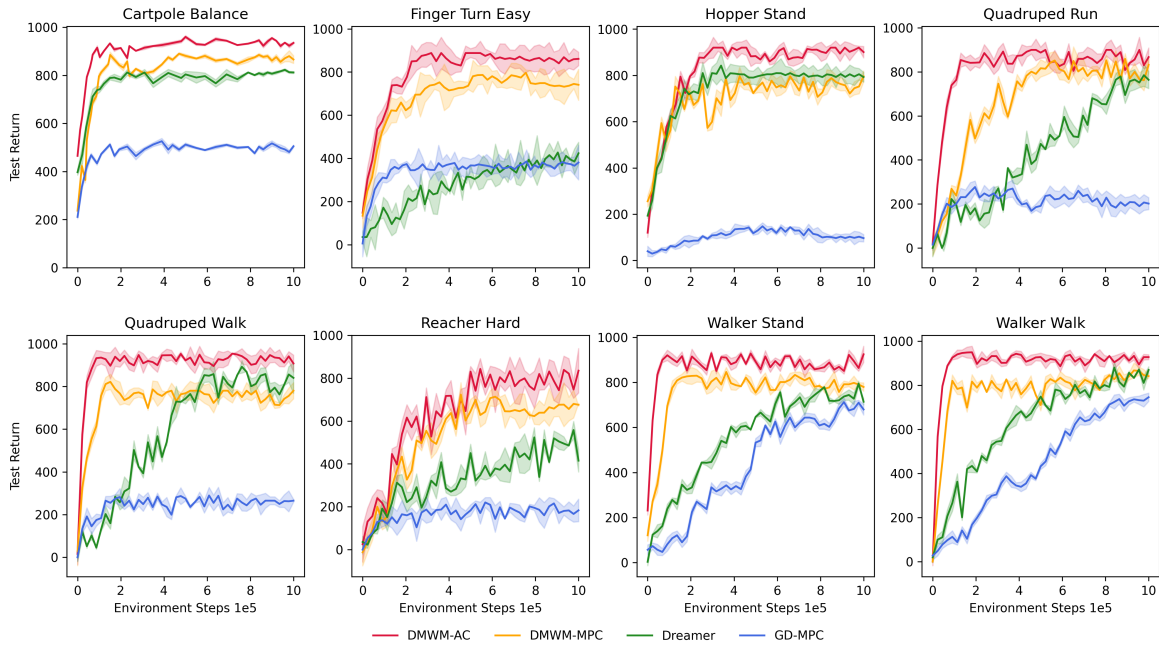


Figure 5. Performance comparison on 8 DMC tasks under limited environment steps, with standard error shaded in the distraction setting. The horizontal axis represents the number of environment interactions, while the vertical axis denotes the average test return over 100 episodes. Complete test results on 20 DMC tasks under limited environment steps are provided in Appendix G.3.

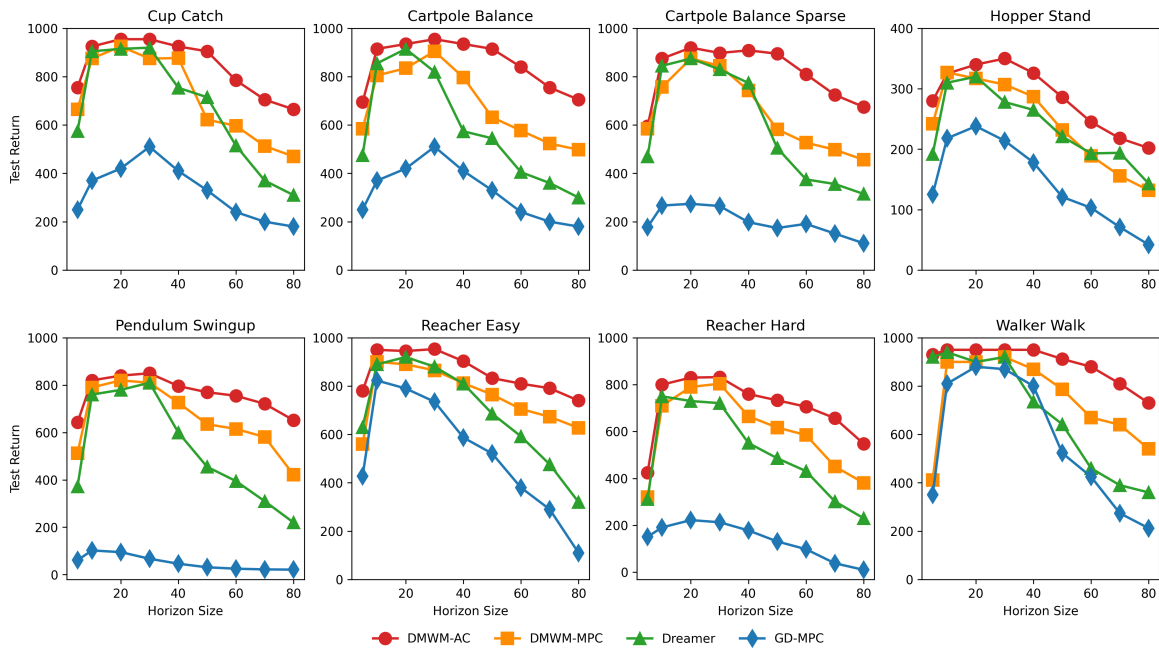


Figure 6. Performance comparison on 8 DMC tasks across different horizon size. The horizontal axis indicates the horizon size. The vertical axis indicates the average test return over 100 episodes. Complete results on 20 DMC tasks across varying horizon size are provided in Appendix G.4.

Limitations and future work. A key limitation of our approach lies in its reliance on predefined simple domain-specific logical rules, which restricts its adaptability to environments where such rules are ambiguous or constantly evolving. This dependency limits the framework’s ability

to generalize to novel tasks. Future work could focus on enabling the model to autonomously learn and adapt logical rules from data by exploring causal relationships. This, in turn, can reduce the need for explicit manual definitions and enhance flexibility in dynamic and complex environments.

Impact Statement

Inspired by the human cognitive model, this paper proposes a novel DMWM architecture that integrates intuitive RSSM-S1 with logic-driven LINN-S2 for the first time, which addresses long-horizon imagination for model-based RL and MPC. By enhancing logical consistency of the architecture, DMWM improves both efficiency and robustness in complex tasks. Because of these benefits, DMWM provides a practical and interpretable solution for real-world applications such as autonomous driving and robotic planning.

Moreover, this work presents a generalized dual-mind framework for world models that can serve as a solid foundation for future research on general world models. We believe this approach marks a meaningful step toward artificial general intelligence (AGI) by bridging intuitive processes with logical reasoning. Hence, DMWM paves the way for more robust, logical and human-like decision-making systems.

References

- Alonso, E., Jelley, A., Micheli, V., Kanervisto, A., Storkey, A., Pearce, T., and Fleuret, F. Diffusion for world modeling: Visual details matter in atari. *arXiv preprint arXiv:2405.12399*, 2024.
- Badreddine, S., Garcez, A. d., Serafini, L., and Spranger, M. Logic tensor networks. *Artificial Intelligence*, 303: 103649, 2022.
- Bruce, J., Dennis, M. D., Edwards, A., Parker-Holder, J., Shi, Y., Hughes, E., Lai, M., Mavalankar, A., Steigerwald, R., Apps, C., et al. Genie: Generative interactive environments. In *Forty-first International Conference on Machine Learning*, 2024.
- Chen, C., Wu, Y.-F., Yoon, J., and Ahn, S. Transdreamer: Reinforcement learning with transformer world models. *arXiv preprint arXiv:2202.09481*, 2022.
- Chen, H., Shi, S., Li, Y., and Zhang, Y. Neural collaborative reasoning. In *Proceedings of the Web Conference 2021*, pp. 1516–1527, 2021.
- Clinton, J. and Lieck, R. Planning transformer: Long-horizon offline reinforcement learning with planning tokens. *arXiv preprint arXiv:2409.09513*, 2024.
- Cohen, L., Wang, K., Kang, B., and Mannor, S. Improving token-based world models with parallel observation prediction. *arXiv preprint arXiv:2402.05643*, 2024.
- Ding, Z., Zhang, A., Tian, Y., and Zheng, Q. Diffusion world model. *arXiv preprint arXiv:2402.03570*, 2024.
- Du, Y., Yang, M., Florence, P., Xia, F., Wahid, A., Ichter, B., Sermanet, P., Yu, T., Abbeel, P., Tenenbaum, J. B., et al. Video language planning. *arXiv preprint arXiv:2310.10625*, 2023.
- Du, Y., Yang, S., Dai, B., Dai, H., Nachum, O., Tenenbaum, J., Schuurmans, D., and Abbeel, P. Learning universal policies via text-guided video generation. *Advances in Neural Information Processing Systems*, 36, 2024.
- Evans, J. S. B. In two minds: dual-process accounts of reasoning. *Trends in cognitive sciences*, 7(10):454–459, 2003.
- Feldstein, J., Dilkas, P., Belle, V., and Tsamoura, E. Mapping the neuro-symbolic ai landscape by architectures: A handbook on augmenting deep learning through symbolic reasoning. *arXiv preprint arXiv:2410.22077*, 2024.
- Feng, Y., Hansen, N., Xiong, Z., Rajagopalan, C., and Wang, X. Finetuning offline world models in the real world. *arXiv preprint arXiv:2310.16029*, 2023.
- Ferreira, J., de Sousa Ribeiro, M., Gonçalves, R., and Leite, J. Looking inside the black-box: Logic-based explanations for neural networks. In *Proceedings of the international conference on principles of knowledge representation and reasoning*, volume 19, pp. 432–442, 2022.
- Frankish, K. Dual-process and dual-system theories of reasoning. *Philosophy Compass*, 5(10):914–926, 2010.
- Garrido, Q., Assran, M., Ballas, N., Bardes, A., Najman, L., and LeCun, Y. Learning and leveraging world models in visual representation learning. *arXiv preprint arXiv:2403.00504*, 2024.
- Georgiev, I., Giridhar, V., Hansen, N., and Garg, A. Pwm: Policy learning with large world models. *arXiv preprint arXiv:2407.02466*, 2024.
- Hafner, D., Lillicrap, T., Ba, J., and Norouzi, M. Dream to control: Learning behaviors by latent imagination. *arXiv preprint arXiv:1912.01603*, 2019a.
- Hafner, D., Lillicrap, T., Fischer, I., Villegas, R., Ha, D., Lee, H., and Davidson, J. Learning latent dynamics for planning from pixels. In *International conference on machine learning*, pp. 2555–2565. PMLR, 2019b.
- Hafner, D., Lillicrap, T., Norouzi, M., and Ba, J. Mastering atari with discrete world models. *arXiv preprint arXiv:2010.02193*, 2020.
- Hafner, D., Pasukonis, J., Ba, J., and Lillicrap, T. Mastering diverse domains through world models. *arXiv preprint arXiv:2301.04104*, 2023.
- Hansen, N., Wang, X., and Su, H. Temporal difference learning for model predictive control. *arXiv preprint arXiv:2203.04955*, 2022.

- Hansen, N., Su, H., and Wang, X. Td-mpc2: Scalable, robust world models for continuous control. *arXiv preprint arXiv:2310.16828*, 2023.
- Hao, S., Gu, Y., Ma, H., Hong, J. J., Wang, Z., Wang, D. Z., and Hu, Z. Reasoning with language model is planning with world model. *arXiv preprint arXiv:2305.14992*, 2023.
- Hu, A., Corrado, G., Griffiths, N., Murez, Z., Gurau, C., Yeo, H., Kendall, A., Cipolla, R., and Shotton, J. Model-based imitation learning for urban driving. *Advances in Neural Information Processing Systems*, 35:20703–20716, 2022.
- Hu, A., Russell, L., Yeo, H., Murez, Z., Fedoseev, G., Kendall, A., Shotton, J., and Corrado, G. Gaia-1: A generative world model for autonomous driving. *arXiv preprint arXiv:2309.17080*, 2023.
- Hua, W. and Zhang, Y. System 1+ system 2= better world: Neural-symbolic chain of logic reasoning. In *Findings of the Association for Computational Linguistics: EMNLP 2022*, pp. 601–612, 2022.
- Kamthe, S. and Deisenroth, M. Data-efficient reinforcement learning with probabilistic model predictive control. In *International conference on artificial intelligence and statistics*, pp. 1701–1710. PMLR, 2018.
- Ke, N. R., Singh, A., Touati, A., Goyal, A., Bengio, Y., Parikh, D., and Batra, D. Modeling the long term future in model-based reinforcement learning. In *International Conference on Learning Representations*, 2018.
- Lambert, N., Wilcox, A., Zhang, H., Pister, K. S., and Calandra, R. Learning accurate long-term dynamics for model-based reinforcement learning. In *2021 60th IEEE Conference on decision and control (CDC)*, pp. 2880–2887. IEEE, 2021.
- LeCun, Y. A path towards autonomous machine intelligence version 0.9. 2, 2022-06-27. *Open Review*, 62(1):1–62, 2022.
- Li, T. and Srikumar, V. Augmenting neural networks with first-order logic. *arXiv preprint arXiv:1906.06298*, 2019.
- Lin, J., Du, Y., Watkins, O., Hafner, D., Abbeel, P., Klein, D., and Dragan, A. Learning to model the world with language. *arXiv preprint arXiv:2308.01399*, 2023.
- Lin, Z., Wu, Y.-F., Peri, S., Fu, B., Jiang, J., and Ahn, S. Improving generative imagination in object-centric world models. In *International conference on machine learning*, pp. 6140–6149. PMLR, 2020.
- Ma, M., Ni, T., Gehring, C., D’Oro, P., and Bacon, P.-L. Do transformer world models give better policy gradients? *arXiv preprint arXiv:2402.05290*, 2024.
- Mattes, P., Schlosser, R., and Herbrich, R. Hieros: Hierarchical imagination on structured state space sequence world models. *arXiv preprint arXiv:2310.05167*, 2023.
- Micheli, V., Alonso, E., and Fleuret, F. Efficient world models with context-aware tokenization. *arXiv preprint arXiv:2406.19320*, 2024.
- Muske, K. R. and Rawlings, J. B. Model predictive control with linear models. *AIChE Journal*, 39(2):262–287, 1993.
- Nottingham, K., Ammanabrolu, P., Suhr, A., Choi, Y., Hajishirzi, H., Singh, S., and Fox, R. Do embodied agents dream of pixelated sheep: Embodied decision making using language guided world modelling. In *International Conference on Machine Learning*, pp. 26311–26325. PMLR, 2023.
- Qu, M. and Tang, J. Probabilistic logic neural networks for reasoning. *Advances in neural information processing systems*, 32, 2019.
- Riegel, R., Gray, A., Luus, F., Khan, N., Makondo, N., Akhalwaya, I. Y., Qian, H., Fagin, R., Barahona, F., Sharma, U., et al. Logical neural networks. *arXiv preprint arXiv:2006.13155*, 2020.
- Rigter, M., Yamada, J., and Posner, I. World models via policy-guided trajectory diffusion. *arXiv preprint arXiv:2312.08533*, 2023.
- Schrittwieser, J., Antonoglou, I., Hubert, T., Simonyan, K., Sifre, L., Schmitt, S., Guez, A., Lockhart, E., Hassabis, D., Graepel, T., et al. Mastering atari, go, chess and shogi by planning with a learned model. *Nature*, 588(7839): 604–609, 2020.
- Sen, P., de Carvalho, B. W., Riegel, R., and Gray, A. Neuro-symbolic inductive logic programming with logical neural networks. In *Proceedings of the AAAI conference on artificial intelligence*, volume 36, pp. 8212–8219, 2022.
- Shi, S., Chen, H., Ma, W., Mao, J., Zhang, M., and Zhang, Y. Neural logic reasoning. In *Proceedings of the 29th ACM International Conference on Information & Knowledge Management*, pp. 1365–1374, 2020.
- Simeonov, A., Du, Y., Kim, B., Hogan, F., Tenenbaum, J., Agrawal, P., and Rodriguez, A. A long horizon planning framework for manipulating rigid pointcloud objects. In *Conference on Robot Learning*, pp. 1582–1601. PMLR, 2021.
- Sun, R., Zang, H., Li, X., and Islam, R. Learning latent dynamic robust representations for world models. *arXiv preprint arXiv:2405.06263*, 2024.
- Sutton, R. S. and Barto, A. G. *Reinforcement learning: An introduction*. MIT press, 2018.

- SV, J., Jalagam, S., LeCun, Y., and Sobal, V. Gradient-based planning with world models. *arXiv preprint arXiv:2312.17227*, 2023.
- Wang, X., Zhu, Z., Huang, G., Chen, X., Zhu, J., and Lu, J. Drivedreamer: Towards real-world-driven world models for autonomous driving. *arXiv preprint arXiv:2309.09777*, 2023.
- Wang, Y., Wan, S., Gan, L., Feng, S., and Zhan, D.-C. Ad3: Implicit action is the key for world models to distinguish the diverse visual distractors. *arXiv preprint arXiv:2403.09976*, 2024.
- Wong, L., Grand, G., Lew, A. K., Goodman, N. D., Mansinghka, V. K., Andreas, J., and Tenenbaum, J. B. From word models to world models: Translating from natural language to the probabilistic language of thought. *arXiv preprint arXiv:2306.12672*, 2023.
- Wu, J., Yin, S., Feng, N., He, X., Li, D., Hao, J., and Long, M. ivideopt: Interactive videopts are scalable world models. *arXiv preprint arXiv:2405.15223*, 2024.
- Wu, P., Escontrela, A., Hafner, D., Abbeel, P., and Goldberg, K. Daydreamer: World models for physical robot learning. In *Conference on robot learning*, pp. 2226–2240. PMLR, 2023.
- Wu, Z., Rincon, D., Gu, Q., and Christofides, P. D. Statistical machine learning in model predictive control of nonlinear processes. *Mathematics*, 9(16):1912, 2021.
- Xiang, J., Liu, G., Gu, Y., Gao, Q., Ning, Y., Zha, Y., Feng, Z., Tao, T., Hao, S., Shi, Y., et al. Pandora: Towards general world model with natural language actions and video states. *arXiv preprint arXiv:2406.09455*, 2024a.
- Xiang, J., Tao, T., Gu, Y., Shu, T., Wang, Z., Yang, Z., and Hu, Z. Language models meet world models: Embodied experiences enhance language models. *Advances in neural information processing systems*, 36, 2024b.
- Ye, W., Liu, S., Kurutach, T., Abbeel, P., and Gao, Y. Mastering atari games with limited data. *Advances in neural information processing systems*, 34:25476–25488, 2021.
- Zhang, L., Xiong, Y., Yang, Z., Casas, S., Hu, R., and Urtasun, R. Learning unsupervised world models for autonomous driving via discrete diffusion. *arXiv preprint arXiv:2311.01017*, 2023.
- Zhen, H., Qiu, X., Chen, P., Yang, J., Yan, X., Du, Y., Hong, Y., and Gan, C. 3d-vla: A 3d vision-language-action generative world model. *arXiv preprint arXiv:2403.09631*, 2024.
- Zhou, S., Du, Y., Chen, J., Li, Y., Yeung, D.-Y., and Gan, C. Robodreamer: Learning compositional world models for robot imagination. *arXiv preprint arXiv:2404.12377*, 2024.
- Zhu, G., Zhang, M., Lee, H., and Zhang, C. Bridging imagination and reality for model-based deep reinforcement learning. *Advances in Neural Information Processing Systems*, 33:8993–9006, 2020.

A. Background

A.1. Actor-Critic

The actor-critic model is a widely used algorithmic framework in Reinforcement Learning (RL), which combines the advantages of policy gradient methods and value function approximation. It addresses RL tasks through the collaborative learning of two primary components: the Actor (policy network) and the Critic (value network), given as follows:

$$\begin{aligned} \text{Action model:} \quad & a_\tau \sim q_\vartheta(a_\tau \mid s_\tau) \\ \text{Value model:} \quad & v_\psi(s_\tau) \approx \mathbb{E}_{q(\cdot \mid s_\tau)} \left(\sum_{t=\tau}^H \gamma^{t-\tau} r_t \right). \end{aligned} \quad (19)$$

In the world Model, the target of the actor-critic model is to maximize the reward over the imagined trajectories with the horizon size H . Specifically, the action model seeks to maximize an estimated value, while the value model strives to accurately predict the value estimate, which evolves as the action model updates. The training target of the Actor and the Value are given as follows (Sutton & Barto, 2018; Hafner et al., 2019a; SV et al., 2023).

$$\vartheta^* = \max_{\vartheta} \mathbb{E}_{q_\phi, q_\vartheta} \left[\sum_{\tau=t}^{t+H} V_\lambda(s_\tau) \right] \quad (20)$$

$$\psi^* = \min_{\psi} \mathbb{E}_{q_\phi, q_\vartheta} \left[\sum_{\tau=t}^{t+H} \frac{1}{2} (v_\psi(s_\tau) - V_\lambda(s_\tau))^2 \right] \quad (21)$$

$$V_\lambda(s_\tau) = (1 - \lambda) \left(\sum_{n=1}^{H-1} \lambda^{n-1} V_n^N(s_\tau) \right) + \lambda^{H-1} V_H^N(s_\tau) \quad (22)$$

$$V_k^N(s_\tau) = \mathbb{E}_{q_\phi, q_\vartheta} \left[\sum_{n=\tau}^{h-1} \gamma^{n-\tau} r_n + \gamma^{h-\tau} v_\psi(s_h) \right], \quad (23)$$

where $h = \min(\tau + k, t + H)$, ϑ represents the parameters of the Actor *psi* represents the parameters of the Critic, and λ is the discount factor.

A.2. Model Predictive Control

Model predictive control (MPC) is an optimization-based control method extensively applied in engineering and industrial control systems (Muske & Rawlings, 1993; Kamthe & Deisenroth, 2018; Wu et al., 2021; Hansen et al., 2023). By leveraging the system's dynamic model, MPC predicts future behavior through rolling optimization, generating optimal control inputs at each time step to achieve the desired system objectives. However, due to the fact that MPC strongly relies on the system model and the requirement for online optimization, it has difficulty in effective decision-making performance if the world model fails to provide stable and reliable imagined trajectories (Hafner et al., 2019b; SV et al., 2023). The gradient-based MPC framework (SV et al., 2023) for world model is presented as

$$a_{t:t+H}^* = \max_{a_{t:t+H}^{(j)}} R^{(j)}, \quad R^{(j)} = \sum_{\tau=t+1}^{t+H+1} \mathbb{E} [q_\phi(r_\tau \mid s_\tau^{(j)})] \quad (24)$$

$$\left\{ a_{t:t+H}^{(j)} \right\}_{j=1}^J \sim \mathcal{N}(\mu_t, \text{diag}(\sigma_t^2)) \quad (25)$$

$$s_{t:t+H+1}^{(j)} \sim q_\phi(s_t \mid o_{1:t}^{(j)}, a_{1:t-1}^{(j)}) \prod_{\tau=t+1}^{t+H+1} p_\phi(s_\tau \mid s_{\tau-1}^{(j)}, a_{\tau-1}^{(j)}) \quad (26)$$

$$a_{t:t+H}^{(j)} = a_{t:t+H}^{(j)} - \nabla R^{(j)}, \quad (27)$$

where $a_{t:t+H}^{(j)}$ and $s_{t:t+H}^{(j)}$ are sequences of states and actions of the candidate j from the timestep t to the timestep $t + H$.

B. Algorithms

B.1. DMWM With Actor-Critic

The training process of DMWM with actor-critic-based decision module is shown in Algorithm 1.

Algorithm 1 DMWM With Actor-Critic

Hyper Parameters: seed episode S , training episodes N , batch size B , collect interval C , sequence length L , imagination horizon H , learning rate η .

Initialize dataset \mathcal{D} with S seed episodes.

Initialize DMWM parameters ϕ, w .

Initialize Actor-Critic parameters ϑ, ψ .

for Training step $n \rightarrow N$ **do**

for Collect interval $c \rightarrow C$ **do**

 // System 1 Training

 Sample B Sequences $\{(o_t, a_t, r_t)\}_{t=k}^{k+L} \sim \mathcal{D}$.

 Compute $h_t = f_\varphi(h_{t-1}, z_{t-1}, a_{t-1})$.

 Predict $\hat{z}_t \sim p_\varphi(\hat{z}_t | h_t), \hat{o}_t \sim p_\varphi(\hat{o}_t | h_t, z_t)$.

 Update S1 $\psi \leftarrow \psi - \eta_\psi \nabla_\psi \mathcal{L}_{S1}(\psi)$.

 // System 2 Training

 Learn Logic Regularizations \mathcal{L}_{reg} .

 // S1's Guidance on S2 Based on Truth $\{(h_t, a_t, h_{t+1})\}$

 Compute $L_T^\lambda = \phi_1^\lambda \wedge \phi_2^\lambda \wedge \phi_3^\lambda \cdots \phi_{T-1}^\lambda$.

 Update S2 $w \leftarrow w - \eta_w \nabla_w \mathcal{L}_{S1}(w)$.

 // Actor-Critic Training

 Imagine $\{(z_\tau, a_\tau)\}_{\tau=t}^{t+H}$ from each z_t .

 Predict rewards $\mathbb{E}(q_\varphi(r_\tau | h_\tau, z_\tau))$ and values $v_\psi(s_\tau)$.

 Compute value estimates $V_\lambda(s_\tau)$.

 Update $\vartheta \leftarrow \vartheta + \eta_\vartheta \nabla_\vartheta \sum_{\tau=t}^{t+H} V_\lambda(s_\tau)$.

 Update $\psi \leftarrow \psi - \eta_\psi \nabla_\psi \sum_{\tau=t}^{t+H} \frac{1}{2} \|v_\psi(s_\tau) - V_\lambda(s_\tau)\|^2$.

 // S2's Guidance on S1 Based on Imagination $\{(z_\tau, a_\tau)\}$

 Compute Logic Consistency of $\{(z_\tau, a_\tau)\}$ With L_T^λ

 Update S1 $\psi \leftarrow \psi - \eta_\psi \nabla_\psi \mathcal{L}_{S2}(\psi)$.

end for

 // Real Environment Interaction & Data Collection

 Start a environment $env.reset()$

for Time step $t \rightarrow T$ **do**

 Compute $h_t = f_\varphi(h_{t-1}, z_{t-1}, a_{t-1})$.

 Compute $z_t \sim q_\varphi(z_t | h_t, o_t)$

 Obtain $a_t \sim q_\vartheta(a_t | z_t)$ from decision-making model.

 Interact $r_t, o_{t+1} \leftarrow env.step(a_t)$.

end for

 Add experience to dataset $\mathcal{D} \leftarrow \mathcal{D} \cup \{(o_t, a_t, r_t)\}_{t=1}^T$.

end for

B.2. DMWM With MPC

The training process of DMWM with Grad-MPC-based decision-making module (SV et al., 2023) is shown in Algorithm 2.

Algorithm 2 DMWM With Grad-MPC

Hyper Parameters: iterations I , candidate Size J , learning rate η_R .
 Initialize dataset \mathcal{D} with S seed episodes.
 Initialize DMWM parameters ϕ, w .
for Training step $n \rightarrow N$ **do**
 ...
 // Real Environment Interaction & Data Collection
 Start a environment $env.reset()$
for Time step $t \rightarrow T$ **do**
 Compute $h_t = f_\phi(h_{t-1}, z_{t-1}, a_{t-1})$.
 Compute $z_t \sim q_\phi(z_t | h_t, o_t)$
 // MPC Decision Making
 Sample Actions $\{a_{t:t+H}^{(j)}\}_{j=1}^J \sim \mathcal{N}(\mu_t, \text{diag}(\sigma_t^2))$.
for Iteration $i \rightarrow I$ **do**
for Candidate sequence $j \rightarrow J$ **do**
 $s_{t:t+H+1}^{(j)} \sim q_\phi(s_t | o_{1:t}, a_{1:t-1}^{(j)}) \prod_{\tau=t+1}^{t+H+1} p_\phi(s_\tau | s_{\tau-1}^{(j)}, a_{\tau-1}^{(j)})$.
 $R^{(j)} = \sum_{\tau=t+1}^{t+H+1} \mathbb{E}[p(r_\tau | s_\tau^{(j)})]$.
 Update Action $a_{t:t+H}^{(j)} = a_{t:t+H}^{(j)} - \eta_R \nabla R^{(j)}$.
end for
end for
 $a_{t:t+H}^* = \max_{a_{t:t+H}^{(j)}} R^{(j)}$
 Interact $r_t, o_{t+1} \leftarrow env.step(a_t^*)$.
end for
 Add experience to dataset $\mathcal{D} \leftarrow \mathcal{D} \cup \{(o_t, a_t, r_t)\}_{t=1}^T$.
 ...
end for

C. Hyperparameters

C.1. Environment Setting

The action repeat setting (Hafner et al., 2019a; SV et al., 2023) of different environments is presented in TABLE 2.

Table 3. Action Repeat Setting

Env	Action Dim	Action Repeat
Cartpole Swingup	1	8
Pendulum Swingup	1	6
Reacher Easy	2	4
Finger Spin	2	2
Cheetah Run	6	4
Cup Catch	2	6
Walker Walk	6	2
Quadruped Walk	12	2
Hopper Hop	4	2

C.2. Model Setting

The hyperparameters of models are presented in TABLE 3.

Table 4. Hyperparameter Setting

Parameter	Symbol	Value
Dual-Mind World Model (General)		
Replay memory size	—	1e6
Batch size	B	50
Sequence length	L	64
Seed episode	S	5
Training episodes	N	1e3
Collect Interval	C	100
Max episode length	—	500
Exploration noise	—	0.3
Imagination horizon	H	30
Gradient clipping	—	100
RSSM-S1		
Activation function	—	Relu
Embedding size	—	1024
Hidden size	—	200
Belief size	—	200
State size	—	30
Overshooting distance	—	50
Overshooting KL-beta	—	0
Global KL-beta	—	0
overshooting reward scale	—	0
Free nats	—	3
Bit-depth	—	5
Weights	$\varpi_{\text{dyn}}, \varpi_{\text{rep}}$	1
Optimizer	—	Adam
Adam epsilon	—	1e-4
Learning rate	η_{ψ}	1e-3
LINN-S2		
Reasoning depth	α	30
Logic vector size	$ v , m $	64
L2 weight	β_{ℓ_2}	1e-5
Regularization weight	β_{reg}	1
Logic MLP number	—	3
Optimizer	—	SGD
Learning rate	η_w	1e-2
Actor-Critic (Hafner et al., 2019a)		
Return lambda	λ	0.95
Planning horizon discount	—	0.99
Optimizer	—	Adam
Adam epsilon	—	1e-4
Learning rate	$\eta_{\theta}, \eta_{\psi}$	1e-4
Grad-MPC (SV et al., 2023)		
Iterations	I	40
Candidate Size	J	1000
Learning Rate	η_R	0.1-0.01-0.005-0.0001

D. Further Related Work

D.1. World Model

World models are fundamental building blocks for model-based intelligent systems to make decisions, learn, and reason in complex environments. It enables prediction, efficient behavior planning through environment simulation, and strategy optimization using virtual simulations, reducing reliance on real-world trial and error (Hafner et al., 2019a; 2020; 2023; Micheli et al., 2024; Zhou et al., 2024). Existing world modeling frameworks can be categorized as Recurrent State-Space Model (RSSM) (Hafner et al., 2019a; 2020; Zhu et al., 2020; Hansen et al., 2022; Hafner et al., 2023; Wu et al., 2023; Lin et al., 2023; Hansen et al., 2023; Feng et al., 2023; Mattes et al., 2023; Sun et al., 2024; Georgiev et al., 2024), Generative Mdoel (Chen et al., 2022; Wang et al., 2023; Hu et al., 2023; Zhang et al., 2023; Rigter et al., 2023; Alonso et al., 2024; Ding et al., 2024; Bruce et al., 2024; Du et al., 2024; Zhen et al., 2024), and Large Language Model (LLM) (Nottingham et al., 2023; Wong et al., 2023; Hao et al., 2023; Wu et al., 2024; Xiang et al., 2024b;a).

The Dreamer series (Hafner et al., 2019a; 2020; 2023) lays an important foundation for general model-based reinforcement learning (MBRL) by continuously improving sample efficiency and task generalization ability through dynamic modeling and planning in the latent space. To adapt the RSSM-based world model for real-world environments, (Zhu et al., 2020) optimized confidence and entropy regularization for the gradient to mitigate discrepancies between virtual simulations and real-world environments. (Lin et al., 2020) studied an object-centric world model, and introduced an object-state recurrent neural network (OS-RNN) to follow the object states. (Du et al., 2024) extended multimodal RSSM to support joint text and visual inputs. (Hafner et al., 2023; Hansen et al., 2023; Georgiev et al., 2024) explored the multiple tasks with RSSM-based world models. (Hansen et al., 2023) utilized SimNorm to sparse and normalize the potential states, which projected the latent representations to simplices of fixed dimensions, thus mitigating the gradient explosion and improving the training stability. (Sun et al., 2024) introduced masking-based latent reconstruction with a dual branch structure to handle the exogenous noise in the complex environment. (Mattes et al., 2023) introduced the hierarchical imagination with parallel processing and proposed efficient time-balanced sampling.

The diffusion model-based world model offers high-quality and diverse generations with temporal smoothness and consistency, achieved through denoising and time inversion processes (Chen et al., 2022; Wang et al., 2023; Hu et al., 2023; Zhang et al., 2023; Rigter et al., 2023; Alonso et al., 2024; Du et al., 2024). However, its reliance on multi-step denoising significantly slows downsampling, inference, and computation compared to RSSM, making it less suitable for real-time tasks and challenging to maintain long-term consistency (Hu et al., 2023; Zhang et al., 2023; Rigter et al., 2023; Du et al., 2024). Additionally, unlike RSSM’s latent space modeling, diffusion models cannot extract task-relevant features and accurately capture environment dynamics, particularly in complex environments with long-tailed distributions (Chen et al., 2022; Hu et al., 2023; Rigter et al., 2023; Ding et al., 2024; Du et al., 2024). The LLM-based world model serves as a powerful tool for complex task planning and execution through its logical reasoning capability and dynamic controllability (Nottingham et al., 2023; Wong et al., 2023; Hao et al., 2023), and is able to realize task decomposition and cross-domain knowledge transfer through natural language instructions (Xiang et al., 2024a). However, the model cannot perform in dynamic modeling, and the generated states and actions often cannot accurately reflect the dynamic changes in the environment. In addition, its high reliance on linguistic representation may lead to insufficient quality of modal alignment, posing the risk of information loss or misinterpretation, while the significant consumption of computational resources during training and inference limits the application of LLM-based world models in resource-constrained environments (Nottingham et al., 2023; Wong et al., 2023; Hao et al., 2023; Wu et al., 2024).

Unlike the aforementioned work, this work focuses on the long-term imagination of world models and proposes to enable the logical consistency of state representations and predictions over an extended horizon for the first time. We retain the efficient sampling and representation capabilities of RSSM as System 1 and integrate a logic-integrated neural network (LINN) as System 2 to imbue the world model with logic reasoning capabilities. The proposed DMWM thus delivers reliable and efficient long-term imagination with logical consistency, addressing a critical research gap in existing approaches.

D.2. Logic Neural Reasoning

Logic neural reasoning enhances the logical consistency, long-term imagination, and generalization ability of world models by embedding logical rules and reasoning capabilities (Ferreira et al., 2022). By combining the interpretability of symbolic logic with the expressive power of neural networks, it provides robust and rapid reasoning for complex task planning (Li & Srikumar, 2019; Qu & Tang, 2019; Shi et al., 2020; Riegel et al., 2020; Chen et al., 2021; Badreddine et al., 2022; Sen et al., 2022). However, explicitly modeling the logical structure of the world presents significant challenges due to the

inherent ambiguity of logical rules, the prevalence of noisy data, and the dynamic and complex nature of logical interactions. (Li & Srikumar, 2019) converted first-order logic rules into computational graphs for neural networks, enhancing their learning capabilities in low-data environments while providing limited support for complex temporal logic. (Qu & Tang, 2019) integrated Markov logic networks with knowledge graph embeddings to address uncertainty in logical reasoning. The logical neural network (LNN) (Riegel et al., 2020) mapped neurons to logical formulas, enabling each neuron to function as a logical operator. However, LNNs rely on predefined and static logical rules, facing limitations in generalization when confronted with uncertainty or evolving logical variables. (Sen et al., 2022) introduced inductive logic programming and automatically learned logic rules. However, the aforementioned approaches make it hard to capture the environment dynamics and extend the long-term imagination capability of the world model. In contrast, the LINN (Shi et al., 2020; Chen et al., 2021) introduces a paradigm shift by dynamically constructing computational graphs and employing neural modules to learn logical operations. Thus, LINN can automatically infer implicit logical rules, circumventing the need for explicit specification. By integrating neural flexibility with logical rigor (Shi et al., 2020; Chen et al., 2021), LINN achieves superior generalization capacity and enhanced robustness to noise, making it well-suited for reasoning tasks in dynamic and complex environments.

This work enhances the long-term imagination capabilities of world models through logical reasoning, a critical yet unexplored area in world model research, with significant implications for advancing Artificial General Intelligence (AGI).

E. Derivation

The ELBO with logic rules for the observation loss can be derived by

$$\begin{aligned}
 \ln p_\varphi(o_{1:T} | a_{1:T}) &= \int p_\varphi(o_{1:T}, z_{1:T} | a_{1:T}) dz_{1:T} \\
 &= \mathbb{E}_{q_\varphi(z_{1:T} | o_{1:T}, a_{1:T})} \left[\frac{p_\varphi(o_{1:T}, z_{1:T} | a_{1:T})}{q_\varphi(z_{1:T} | o_{1:T}, a_{1:T})} \right] \\
 &= \ln \mathbb{E}_{q_\varphi(z_{1:T} | o_{1:T}, a_{1:T})} \left[\prod_{t=1}^T \frac{p_\varphi(o_t | z_t) p_\varphi(z_t | z_{t-1}, a_{t-1}) \mathcal{C}(\phi(z_t, z_{t-1}, a_{t-1}))}{q_\varphi(z_t | o_{\leq t}, a_{\leq t})} \right] \\
 &\geq \mathbb{E}_{q_\varphi(z_{1:T} | o_{1:T}, a_{1:T})} \left[\sum_{t=1}^T \ln p_\varphi(o_t | z_t) + \ln p_\varphi(z_t | z_{t-1}, a_{t-1}) \right. \\
 &\quad \left. + \ln \mathcal{C}(\phi(z_t, z_{t-1}, a_{t-1}) - \ln q_\varphi(z_t | o_{\leq t}, a_{\leq t})) \right] \\
 &= \sum_{t=1}^T \left(\underbrace{\mathbb{E}_{q_\varphi(z_t | o_{\leq t}, a_{\leq t})} [\ln p_\varphi(o_t | z_t)]}_{\text{Decoding}} + \underbrace{\mathbb{E}_{q_\varphi(z_t | o_{\leq t}, a_{\leq t})} [\ln \mathcal{C}(\phi(z_t, z_{t-1}, a_{t-1}))]}_{\text{Logic Inference}} \right. \\
 &\quad \left. - \underbrace{\mathbb{E}_{q_\varphi(z_{t-1} | o_{\leq t-1}, a_{\leq t-1})} [\text{KL}[q_\varphi(z_t | o_{\leq t}, a_{\leq t}) || p_\varphi(z_t | z_{t-1}, a_{t-1})]}]}_{\text{Prediction}} \right)
 \end{aligned} \tag{28}$$

F. Complete Logic Regularization and Rules Table

The complete logic rules and the corresponding regularizers are given in TABLE 5 (Shi et al., 2020).

Table 5. Complete Logical Regularizers and Rules for System 2

	Logical Rule	Equation	Logic Regularizer r_i
NOT	Negation	$w \rightarrow \mathbf{T} = \mathbf{T}$	$r_1 = \sum_{w \in W \cup \{\mathbf{T}\}} \text{Sim}(\text{NOT}(w), w)$
	Double Negation	$\neg(\neg w) = w$	$r_2 = \sum_{w \in W} 1 - \text{Sim}(\text{NOT}(\text{NOT}(w)), w)$
AND	Identity	$w \wedge \mathbf{T} = w$	$r_3 = \sum_{w \in W} 1 - \text{Sim}(\text{AND}(w, \mathbf{T}), w)$
	Annihilator	$w \wedge \mathbf{T} = w$	$r_4 = \sum_{w \in W} 1 - \text{Sim}(\text{AND}(w, \mathbf{F}), \mathbf{F})$
	Idempotence	$w \wedge \mathbf{F} = \mathbf{F}$	$r_5 = \sum_{w \in W} 1 - \text{Sim}(\text{AND}(w, w), w)$
	Complementation	$w \wedge w = w$	$r_6 = \sum_{w \in W} 1 - \text{Sim}(\text{AND}(w, \text{NOT}(w)), \mathbf{F})$
OR	Identity	$w \vee \mathbf{F} = w$	$r_7 = \sum_{w \in W} 1 - \text{Sim}(\text{OR}(w, \mathbf{F}), w)$
	Annihilator	$w \vee \mathbf{T} = \mathbf{T}$	$r_8 = \sum_{w \in W} 1 - \text{Sim}(\text{OR}(w, \mathbf{T}), \mathbf{T})$
	Idempotence	$w \vee w = w$	$r_9 = \sum_{w \in W} 1 - \text{Sim}(\text{OR}(w, w), w)$
	Complementation	$w \vee \neg w = \mathbf{T}$	$r_{10} = \sum_{w \in W} 1 - \text{Sim}(\text{OR}(w, \text{NOT}(w)), \mathbf{T})$
IMPLY	Identity	$w \rightarrow \mathbf{T} = \mathbf{T}$	$r_{11} = \sum_{w \in W} 1 - \text{Sim}(\text{OR}(\text{NOT}(w), \mathbf{T}), \mathbf{T})$
	Annihilator	$w \rightarrow \mathbf{F} = \neg w$	$r_{12} = \sum_{w \in W} 1 - \text{Sim}(\text{OR}(\text{NOT}(w), \mathbf{F}), \text{NOT}(w))$
	Idempotence	$w \rightarrow w = \mathbf{T}$	$r_{13} = \sum_{w \in W} 1 - \text{Sim}(\text{OR}(\text{NOT}(w), w), \mathbf{T})$
	Complementation	$w \rightarrow \neg w \equiv \neg w$	$r_{14} = \sum_{w \in W} 1 - \text{Sim}(\text{OR}(\text{NOT}(w), \text{NOT}(w)), \text{NOT}(w))$

G. Additional Experiments

G.1. Logical Consistency

Table 6. Logical consistency comparison between our proposed DMWM and various RSSM baselines across 20 DMC tasks. We report the mean and variance of logical consistency from imagination over 100 test episodes with the horizon size of $H = 10, 30, 50, 100$.

Env	Horizon Size	Dreamer	Hieros	HRSSM	DMWM (Ours)
Acrobot Swingup	10	0.713 \pm 0.031	0.730 \pm 0.012	0.722 \pm 0.017	0.733 \pm 0.007
	30	0.667 \pm 0.063	0.704 \pm 0.032	0.712 \pm 0.044	0.731 \pm 0.017
	50	0.568 \pm 0.129	0.692 \pm 0.058	0.687 \pm 0.083	0.715 \pm 0.032
	100	0.485 \pm 0.167	0.672 \pm 0.112	0.651 \pm 0.132	0.699 \pm 0.078
Cartpole Balance	10	0.721 \pm 0.023	0.730 \pm 0.009	0.729 \pm 0.011	0.730 \pm 0.008
	30	0.683 \pm 0.057	0.711 \pm 0.032	0.713 \pm 0.041	0.727 \pm 0.023
	50	0.574 \pm 0.112	0.687 \pm 0.084	0.695 \pm 0.072	0.717 \pm 0.045
	100	0.491 \pm 0.171	0.663 \pm 0.142	0.655 \pm 0.121	0.701 \pm 0.092
Cartpole Balance Sparse	10	0.705 \pm 0.132	0.719 \pm 0.032	0.722 \pm 0.034	0.722 \pm 0.026
	30	0.602 \pm 0.167	0.682 \pm 0.101	0.693 \pm 0.081	0.695 \pm 0.093
	50	0.432 \pm 0.203	0.632 \pm 0.178	0.643 \pm 0.162	0.652 \pm 0.135
	100	0.321 \pm 0.286	0.571 \pm 0.232	0.589 \pm 0.213	0.603 \pm 0.182
Cartpole Swingup	10	0.719 \pm 0.031	0.729 \pm 0.011	0.723 \pm 0.023	0.730 \pm 0.011
	30	0.678 \pm 0.062	0.698 \pm 0.043	0.703 \pm 0.082	0.723 \pm 0.032
	50	0.563 \pm 0.091	0.672 \pm 0.124	0.662 \pm 0.145	0.702 \pm 0.078
	100	0.474 \pm 0.158	0.621 \pm 0.191	0.602 \pm 0.191	0.672 \pm 0.152
Cartpole Swingup Sparse	10	0.703 \pm 0.142	0.717 \pm 0.036	0.715 \pm 0.052	0.720 \pm 0.030
	30	0.613 \pm 0.187	0.669 \pm 0.121	0.671 \pm 0.098	0.699 \pm 0.087
	50	0.443 \pm 0.213	0.621 \pm 0.185	0.621 \pm 0.173	0.669 \pm 0.121
	100	0.403 \pm 0.252	0.532 \pm 0.241	0.559 \pm 0.231	0.627 \pm 0.162
Cheetah Run	10	0.709 \pm 0.085	0.723 \pm 0.031	0.721 \pm 0.023	0.730 \pm 0.016
	30	0.643 \pm 0.131	0.689 \pm 0.113	0.695 \pm 0.087	0.725 \pm 0.049
	50	0.527 \pm 0.165	0.651 \pm 0.147	0.667 \pm 0.131	0.703 \pm 0.092
	100	0.428 \pm 0.221	0.606 \pm 0.186	0.627 \pm 0.183	0.676 \pm 0.142
Cup Catch	10	0.711 \pm 0.049	0.728 \pm 0.010	0.726 \pm 0.014	0.732 \pm 0.008
	30	0.652 \pm 0.087	0.701 \pm 0.072	0.714 \pm 0.061	0.728 \pm 0.021
	50	0.534 \pm 0.113	0.681 \pm 0.098	0.683 \pm 0.112	0.712 \pm 0.053
	100	0.465 \pm 0.181	0.647 \pm 0.182	0.633 \pm 0.172	0.692 \pm 0.112

DMWM: Dual-Mind World Model with Long-Term Imagination

Finger Spin	10	0.712 ± 0.075	0.727 ± 0.011	0.728 ± 0.017	0.733 ± 0.009
	30	0.647 ± 0.102	0.705 ± 0.052	0.712 ± 0.057	0.729 ± 0.017
	50	0.517 ± 0.131	0.687 ± 0.091	0.679 ± 0.136	0.710 ± 0.062
	100	0.435 ± 0.211	0.636 ± 0.165	0.645 ± 0.185	0.684 ± 0.127
Finger Turn Easy	10	0.708 ± 0.098	0.726 ± 0.013	0.724 ± 0.018	0.732 ± 0.015
	30	0.634 ± 0.113	0.702 ± 0.051	0.705 ± 0.067	0.728 ± 0.023
	50	0.512 ± 0.157	0.681 ± 0.117	0.682 ± 0.132	0.712 ± 0.067
	100	0.412 ± 0.191	0.644 ± 0.194	0.617 ± 0.197	0.683 ± 0.148
Finger Turn Hard	10	0.704 ± 0.118	0.723 ± 0.014	0.724 ± 0.021	0.731 ± 0.011
	30	0.627 ± 0.131	0.698 ± 0.061	0.703 ± 0.073	0.725 ± 0.029
	50	0.487 ± 0.162	0.673 ± 0.112	0.673 ± 0.152	0.705 ± 0.073
	100	0.385 ± 0.231	0.623 ± 0.201	0.601 ± 0.205	0.675 ± 0.142
Hopper Hop	10	0.703 ± 0.092	0.729 ± 0.023	0.726 ± 0.023	0.731 ± 0.017
	30	0.633 ± 0.127	0.704 ± 0.087	0.701 ± 0.092	0.722 ± 0.038
	50	0.506 ± 0.191	0.664 ± 0.132	0.673 ± 0.132	0.698 ± 0.092
	100	0.407 ± 0.237	0.612 ± 0.237	0.623 ± 0.201	0.689 ± 0.143
Hopper Stand	10	0.709 ± 0.056	0.728 ± 0.021	0.725 ± 0.019	0.732 ± 0.013
	30	0.645 ± 0.112	0.699 ± 0.057	0.704 ± 0.081	0.724 ± 0.039
	50	0.523 ± 0.168	0.671 ± 0.121	0.689 ± 0.137	0.703 ± 0.080
	100	0.421 ± 0.197	0.632 ± 0.211	0.642 ± 0.189	0.692 ± 0.139
Pendulum Swingup	10	0.715 ± 0.054	0.728 ± 0.017	0.719 ± 0.023	0.732 ± 0.015
	30	0.611 ± 0.137	0.709 ± 0.054	0.699 ± 0.079	0.730 ± 0.037
	50	0.526 ± 0.161	0.684 ± 0.112	0.664 ± 0.146	0.721 ± 0.088
	100	0.359 ± 0.224	0.641 ± 0.198	0.612 ± 0.204	0.686 ± 0.131
Quadruped Run	10	0.718 ± 0.042	0.727 ± 0.023	0.725 ± 0.019	0.731 ± 0.013
	30	0.642 ± 0.107	0.701 ± 0.072	0.702 ± 0.074	0.726 ± 0.042
	50	0.556 ± 0.143	0.679 ± 0.135	0.683 ± 0.137	0.705 ± 0.078
	100	0.398 ± 0.217	0.644 ± 0.193	0.629 ± 0.184	0.682 ± 0.129
Quadruped Walk	10	0.719 ± 0.045	0.728 ± 0.027	0.724 ± 0.017	0.732 ± 0.011
	30	0.656 ± 0.092	0.701 ± 0.067	0.703 ± 0.072	0.723 ± 0.039
	50	0.534 ± 0.129	0.682 ± 0.114	0.685 ± 0.132	0.701 ± 0.082
	100	0.413 ± 0.212	0.654 ± 0.183	0.634 ± 0.179	0.687 ± 0.137
Reacher Easy	10	0.711 ± 0.065	0.729 ± 0.012	0.724 ± 0.013	0.732 ± 0.008
	30	0.634 ± 0.102	0.706 ± 0.061	0.705 ± 0.067	0.731 ± 0.031
	50	0.464 ± 0.167	0.675 ± 0.104	0.678 ± 0.121	0.720 ± 0.075
	100	0.373 ± 0.221	0.631 ± 0.175	0.614 ± 0.163	0.705 ± 0.125
Reacher Hard	10	0.712 ± 0.072	0.729 ± 0.013	0.724 ± 0.014	0.732 ± 0.010
	30	0.608 ± 0.121	0.702 ± 0.062	0.703 ± 0.072	0.730 ± 0.042
	50	0.501 ± 0.189	0.663 ± 0.114	0.674 ± 0.132	0.717 ± 0.082
	100	0.349 ± 0.233	0.602 ± 0.183	0.607 ± 0.172	0.701 ± 0.165
Walker Run	10	0.702 ± 0.137	0.720 ± 0.023	0.713 ± 0.027	0.729 ± 0.013
	30	0.554 ± 0.158	0.676 ± 0.067	0.682 ± 0.092	0.711 ± 0.072
	50	0.424 ± 0.213	0.613 ± 0.132	0.658 ± 0.188	0.672 ± 0.128
	100	0.323 ± 0.261	0.532 ± 0.191	0.572 ± 0.243	0.645 ± 0.175
Walker Stand	10	0.706 ± 0.087	0.728 ± 0.012	0.721 ± 0.012	0.734 ± 0.008
	30	0.598 ± 0.128	0.690 ± 0.051	0.692 ± 0.113	0.722 ± 0.067
	50	0.494 ± 0.173	0.648 ± 0.108	0.658 ± 0.162	0.701 ± 0.138
	100	0.369 ± 0.241	0.568 ± 0.172	0.572 ± 0.221	0.662 ± 0.185
Walker Walk	10	0.701 ± 0.118	0.727 ± 0.015	0.723 ± 0.022	0.731 ± 0.028
	30	0.612 ± 0.140	0.696 ± 0.063	0.701 ± 0.073	0.730 ± 0.034
	50	0.474 ± 0.181	0.664 ± 0.123	0.667 ± 0.112	0.718 ± 0.079
	100	0.371 ± 0.251	0.598 ± 0.194	0.601 ± 0.171	0.675 ± 0.142

G.2. Data Efficiency

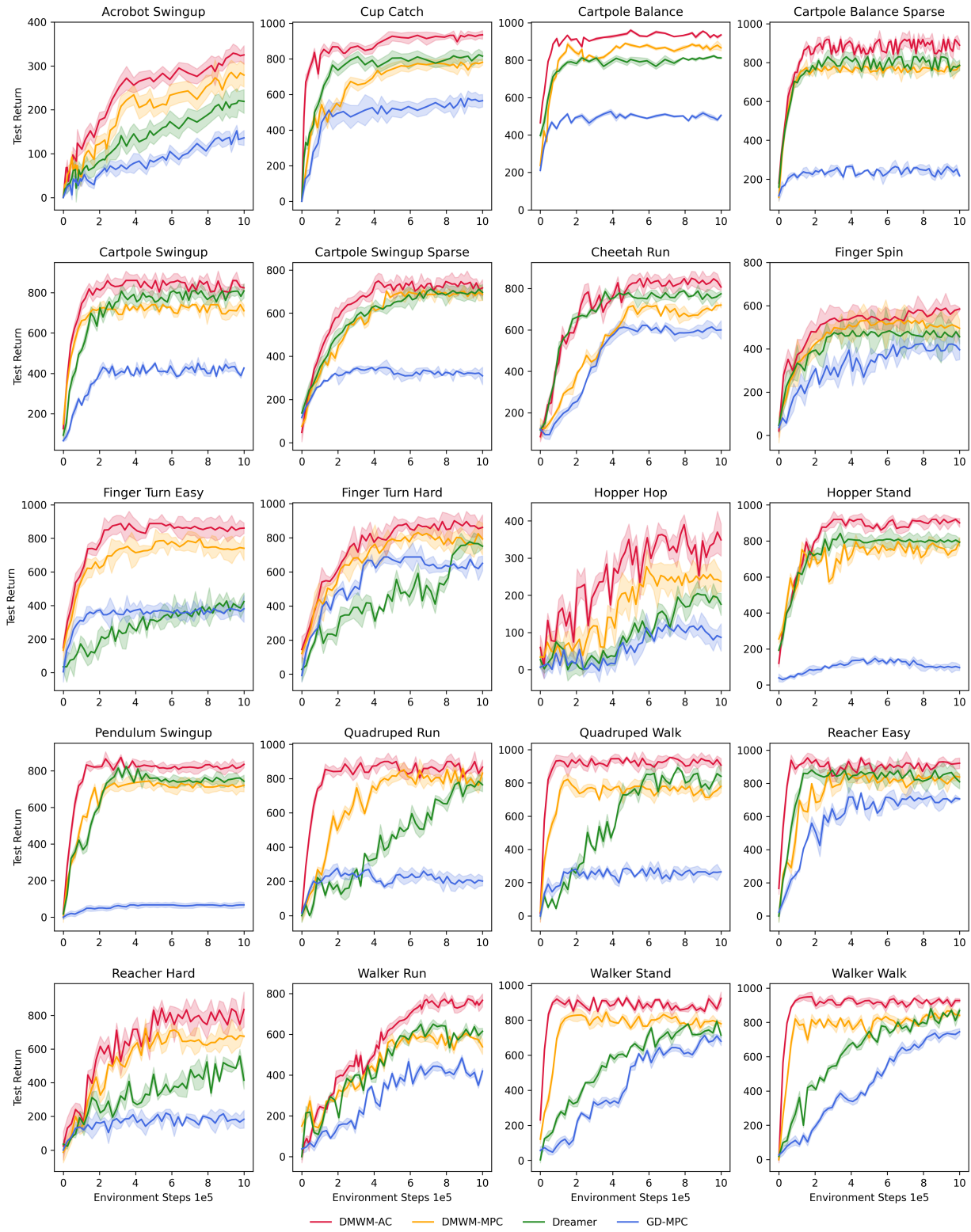


Figure 7. Performance comparison of test results on 20 DMC tasks under limited environment interactions, where the standard error is shaded in the distraction setting. The horizontal axis indicates the number of times that the models explore the environments. The vertical axis represents the average test return over 100 test episodes.

G.3. Trial Efficiency

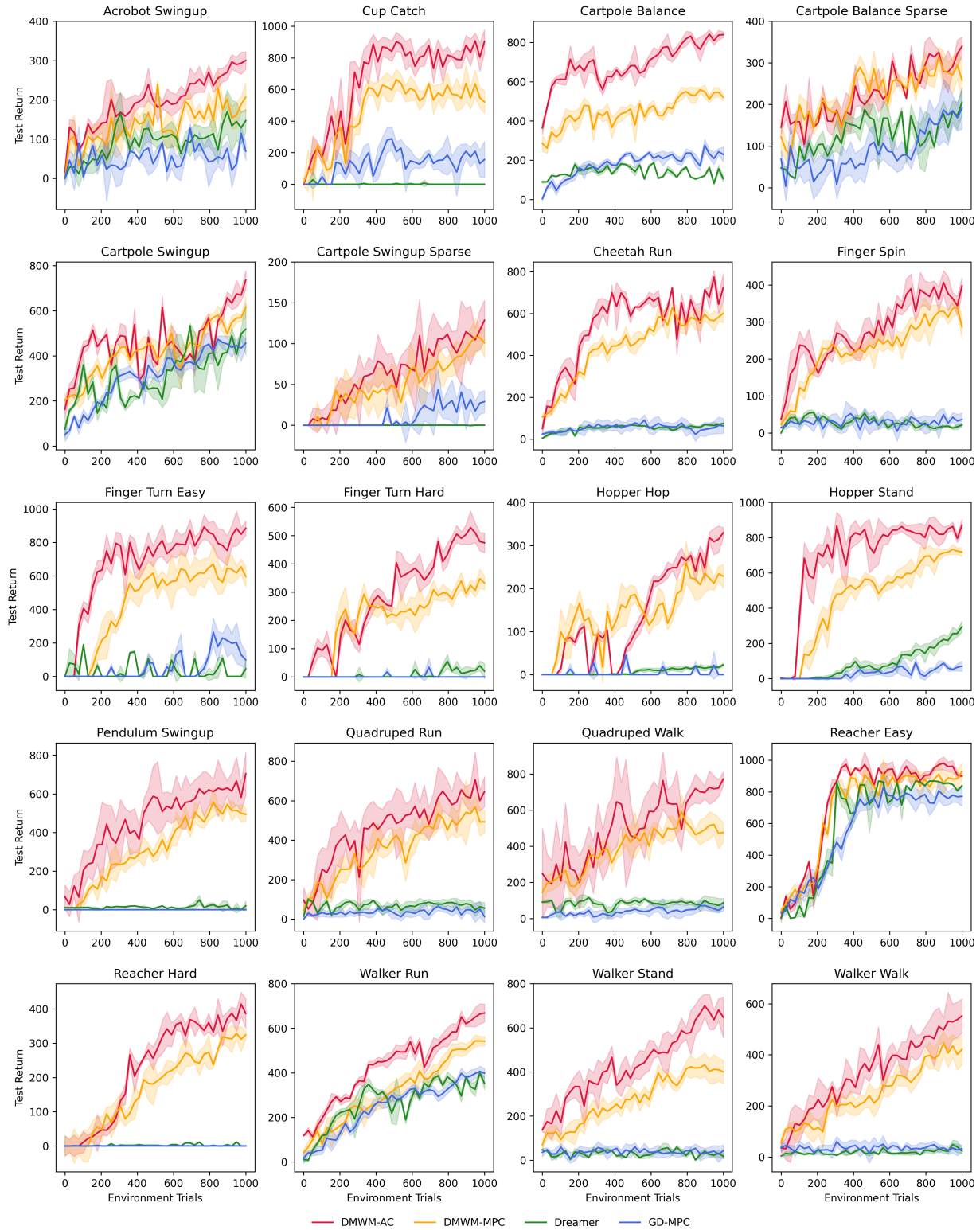


Figure 8. Performance comparison of test results on 20 DMC tasks under limited environment steps, where the standard error is shaded in the distraction setting. The horizontal axis indicates the number of environment data that is used to train the models. The vertical axis represents the average test return over 100 test episodes.

G.4. Long-term Imaginations Over Extended Horizon Size

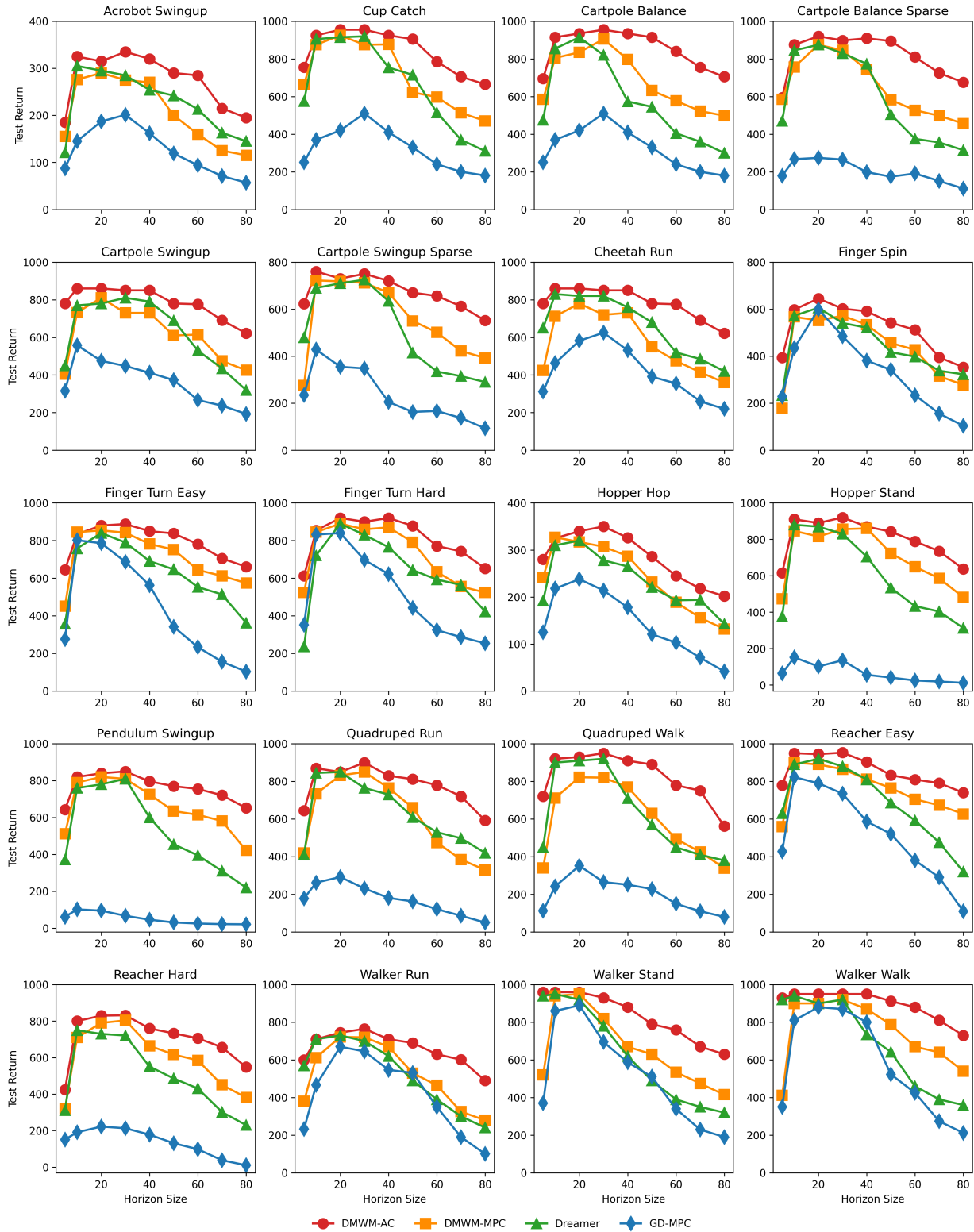


Figure 9. Performance comparison of test results on 20 DMC tasks over different horizon size of imagination. The horizontal axis indicates the horizon size of each imagination. The vertical axis represents the average test return over 100 test episodes.